RSCPublishing

Cite this: DOI: 10.1039/x0xx00000x

www.rsc.org/

ARTICLE

Chalcogenodiazolo[3,4-*c*]pyridine based Donor-Acceptor-Donor Polymers for Green and Near-Infrared Electrochromics

Shouli Ming, Shijie Zhen, Ximei Liu, Kaiwen Lin, Hongtao Liu, Yao Zhao, Baoyang Lu* and Jingkun Xu*

Received (in XXX, XXX) Xth XXXXXXXXX 20XX, Accepted Xth XXXXXXXXX 20XX

A series of thiadiazolo[3,4-*c*]pyridine (PT)/selenadiazolo[3,4-*c*]pyridine (PSe) in alternation with a variety of thiophenes including thiophene (Th), 3-methylthiophene (MeTh), 3-hexylthiophene (HexTh) and 3,4-ethoxylenedioxythiophene (EDOT) based donor-acceptor-donor (D-A-D) monomers were designed and electropolymerized to yield their corresponding polymers. The structure-property relationships of these monomers/polymers, including band gap, electrochemical behavior, and optical properties, were comparatively investigated. The monomers exhibited orange, red, and purple emission characteristics with quantum yields ranging from 0.072 to 0.849 and could probably be used as building blocks for rational design of fluorescent materials. Also, it was noted that these donor and acceptor units played key roles on the optical absorption, leading to the neutral electrochromic polymers with different colors including green, purple, gray, sky blue and dark blue. In particular, the obtained EDOT based polymers revealed obvious color change from green to blue with faster response time (0.3~0.6 s) relative to its analogue benzochalcogenodiazole system. Furthermore, the thiophene and alkyl thiophene based polymers kept their color constant under different applied voltages and showed superior optical contrast (~37%) in the near-infrared region compared with that in the visible region. These intriguing features of polymeric materials demonstrated that inserting chalcogenodiazolo[3,4-*c*]pyridine into D-A-D system allowed green and near-infrared electrochromes.

1. Introduction

Conjugated polymers exhibit several advantages in the field of electrochromism such as the flexibility of color modification, high optical contrast ratio, long-term stability and superior coloration efficiency, which makes them good candidates for the electrochromic applications, such as smart windows, mirrors, optical displays, and camouflage materials.[1-6] On this account, remarkable effort has been devoted to achieving excellent electrochromic polymers in order to meet the requirement for commercial applications.

Color change, an important criterion of electrochromic polymers, is always regarded as a challenging target for the research personnel.[1,4-8] According to color maxing theory, all colors can be achieved through assembling the three complementary colors including red, green and blue. Unfortunately, most electrochromic polymers reported so far display the red and blue color, and only a few polymers exhibit green color at unpredictable state.[7-9] To obtain the complementary green color, there should be at least two absorption bands located in red and blue region, and these bands should deplete in the oxidized state. The critical requirement still makes the green polymers meager in the field of electrochromism. Up to date, these methods adjusting the color of electrochromic polymer consist of using donor-acceptor (D-A) structure, increasing conjugated chain, and employing steric interaction, *etc*. However, the shortcut for achieving the rare green leg of RGB (red-green-blue) color space is currently limited to D-A structure. Also, the first green electrochromic polymer came by Wudl *et al*[11] shows the feasibility and veracity of this approach. Soon after this pioneering work, Reynolds and Toppare groups[12-30] further develop this topic by synthesizing D-A green and black electrochromic polymers based on benzothiadiazole derivatives/analogues as novel acceptor unit along the polymer backbone. Considering the important role of green electrochromic polymers in modulating the color, the species are far from prosperity and still have significant scope for development.

Besides the green color in electrochromics, while extensive studies have been focused on color transitions in the visible range, very little has been done to characterize the near-infrared

---

School of Pharmacy, Jiangxi Science & Technology Normal University, Nanchang 330013, China
Email: lby1258@163.com, xujingkun@tsinghua.org.cn;
Tel: +86-791-88537967, Fax: +86-791-83823320;

†Electronic supplementary information (ESI) available: ^{1}H and ^{13}C NMR spectra for target monomers; FT-IR spectra and detailed peak assignments for the monomers and polymers; anodic polarization curves of monomers; electrochromic parameters of these PT/PSe based polymers. See DOI: 10.1039/x0xx000000x/.

electrochromics. For some specific applications, such as military camouflage and thermal emission detector for spacecraft,[4,31] a unique characteristic is very essential for these near-infrared electrochromic polymers besides the advantage of lightweight, *i. e.*, the response in the near-infrared region but no optical changes in the visible region. Unfortunately, the previously reported near-infrared electrochromic polymers show profound contrast ratios in the visible region and exhibit obvious color change between the neutral and oxidized state, which hinders the development of their promising applications. In view of this situation, the development of novel electrochromic polymers with properties sufficing for these relevant applications are very necessary and significant, and apparently also a considerable challenge.

On the other hand, in these peculiar (green, black and near-infrared) electrochromic polymer family, in sharp contrast to benzothiadiazole derivatives/analogues extensively employed as the acceptor units, the research of thiadiazolo[3,4-*c*]pyridine (PT) has just been established most recently. Due to stronger electron-withdrawing ability of pyridine ring, PT based donor-acceptor-type polymers exhibited several special properties and advantages in the field of organic electronics, such as lower band gap, deeper HOMO-LUMO levels, and improved short-circuit currents.[32-36] Inspired by excellent optoelectronic properties of these PT-based conjugated polymers, our group extended this research to the electrochromics of PT based polymer (PEDOT-PT) recently.[35] With one nitrogen atom substituted onto the benzene ring, the modified polymer still revealed green color at the reduced state, and exhibited decreased bandgap, faster switching time and higher coloration efficiency, as compared with those of the benzothiadiazole (BT) analogue. Significantly, PEDOT-PT showed inferior optical contrast in visible region relative to that in near-infrared region, which inspired us to further explore the availability of PT in the field of near-infrared electrochromics. To these purposes, we wish to undertake an approach that combines PT with various thiophene derivatives bearing different alkyl chains. This approach not only gives the opportunity to understand the effect of the donor units on the electrochromic performance of these D-A-D systems, but also views the modulation of color through substituents and steric interactions.

Furthermore, it is predicted that the heteroatom substitution in similar systems can affect the electrochemical and optoelectronic properties of conjugated structures.[37,38] Therefore, it can be reasonably deduced that selenadiazolo[3,4-*c*]pyridine (PSe), a new acceptor by replacing the sulfur atom (S) in PT unit with selenium atom (Se), would probably be a promising acceptor. There are also several other facts contributing to this hypothesis: (1) with lower electronegativity, larger atomic size and more polarizability of Se than S, Se-based systems are electron richer compared with S-based systems;[37,39] (2) Se-based polymers exhibit several unique features, such as excellent optical and oxidative stability, stronger intermolecular interactions and more quinoid characteristic;[37,38] (3) Se-based D-A-D polymers should have lower band gaps than PT-based analogues due to the stabilization of LUMO levels,[43] which is quite beneficial to tune the color of the corresponding polymers.

Herein, to explore novel conjugated units for rational design of green and near-infrared electrochromic polymers, a series of novel D-A-D monomers with PT/PSe as the acceptor were synthesized, and then electropolymerized in order to form their corresponding polymers (Scheme 1). The structure-property relationships of these monomers and polymers, including optical and electrochemical properties, spectroelectrochemistry and electrochromics, were systematically explored.

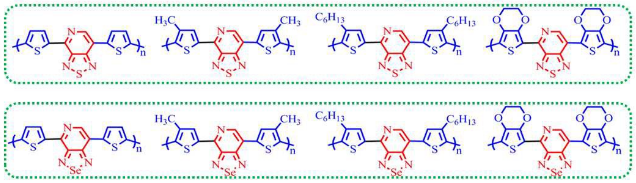

Scheme 1 The synthesized D-A-D conjugated polymers with PT/PSe as the acceptor units.

2. Experimental

2.1 Materials

3,4-Ethylenedioxythiophene (EDOT, 98%; Sigma-Aldrich), thiophene (Th, 99%; *J&K* chemical Ltd), 3-methylthiophene (MeTh, 99%; *J&K* chemical Ltd), 3-hexylthiophene (HexTh, 99%; *J&K* chemical Ltd), 2,3-diaminopyridine (98%; Shanghai Vita Chemical Reagent Co., Ltd), selenium dioxide (SeO_2, 98%; Energy Chemical), thionyl bromide ($SOBr_2$, 97%; *J&K* chemical Ltd), hydrobromic acid (HBr, 48%; *J&K* chemical Ltd), *n*-butyllithium (*n*-BuLi, 2.5 mol L^{-1} in hexanes; Energy Chemical), chlorotributyltin ($SnBu_3Cl$, Energy Chemical), tetrakis (triphenylphosphine)palladium (0) ($Pd(PPh_3)_4$, 99%; Energy Chemical), trans-dichlorobis(triphenyl-phosphine)palladium (II) ($Pd(PPh_3)_2Cl_2$, 99%; Energy Chemical) and acetonitrile (MeCN, 99.9%; Xilong Chemical) were used directly without further purification. Tetrabutylammonium hexafluorophosphate (Bu_4NPF_6, 98%; Energy Chemical) was dried under vacuum at 60 °C for 24 h before use. Tetrahydrofuran (THF, analytical grade; Xilong Chemical), dimethylformamide (DMF, analytical grade; Xilong Chemical) and dichloromethane (CH_2Cl_2, analytical grade; Shanghai Vita Chemical Reagent Co., Ltd) were purified by distillation with calcium hydride under a nitrogen atmosphere before use. Other reagents were all analytical grade and used as received without further treatment.

2.2 Characterization

^1H NMR and ^{13}C NMR spectra were recorded on a Bruker AV 400 NMR spectrometer with $CDCl_3$ or DMSO-d_6 as the solvent and tetramethylsilane as an internal standard (TMS, singlet, chemical shift: 0.0 ppm). UV-vis spectra of the monomers and polymers were taken by using SPECORD 200 PLUS UV-vis spectrophotometer. With an F-4500 fluorescence spectrophotometer (Hitachi), the fluorescence spectra of the monomers were determined. Infrared spectra were determined with a Bruker Vertex 70 Fourier-transform infrared (FT-IR) spectrometer with samples in KBr pellets.

2.3 Monomer synthesis

The synthesis of monomers was shown in Scheme 2. Tributyl(2,3-dihydrothieno[3,4-*b*][1,4]dioxin-5-yl)stannane, tributyl(thiophen-2-yl)stannane (10a), tributyl(4-methylthiophen-2-yl)stannane (10b), tributyl(4-hexylthiophen-2-yl)stannane

(10c), and 4,7-dibromo-[1,2,5]thiadiazolo[3,4-*c*]pyridine (11a) were synthesized according to the reported procedures.[33-35,41]

2.3.1 4,7-Dibromo-[1,2,5]selenadiazolo[3,4-*c*]pyridine (11b). 2,5-Dibromo-3,4-diaminopyridine (1.00 g, 3.74 mmol) and ethanol (15.0 mL) were added to a two-neck 50.0 mL round-bottom flask and heated to reflux with stirring. After slowly adding a solution of selenium dioxide (0.420 g, 3.75 mmol) in ethanol, the reaction mixture was refluxed for 8 h and cooled to room temperature. Then, the solvent was removed by filtration, and the product was washed with ethanol (50.0 mL) to obtain 0.760 g of a light green solid (Yield: 59.0%). ^{1}H NMR (400 MHz, $CDCl_3$, ppm): 8.40 (s, 1H). ^{13}C NMR (400 MHz, $CDCl_3$, ppm): 158.62, 154.62, 144.41, 139.83, 114.43.

2.3.2 Representative procedures for the synthesis of 1-2. To a nitrogen-degassed solution of 2-tributylstannyl-3,4-ethylenedioxythiophene (2.67 g, 6.20 mmol) and 11a or 11b (1.55 mmol) in dry DMF (25.0 mL) was added Pd(PPh$_3$)$_4$ (0.179 g, 0.155 mmol) and then the mixture was stirred at 95 °C for 24 h. After being cooled to room temperature, the mixture was poured into saturated aqueous brine and then extracted with dichloromethane (3 × 20.0 ml). The organic layer was washed twice with water, dried over anhydrous $MgSO_4$ and purified by silica column chromatography. Finally, the crude product was purified by reprecipitation several times, affording the product as a crystal.

EDOT-PT (1). 81.0% yield. ^{1}H NMR (400 MHz, DMSO-d_6, ppm): δ 9.23 (s, 1H), 7.05 (s, 1H), 6.93 (s, 1H), 4.46 (s, 2H), 4.38 (s, 2H), 4.32 (s, 4H); ^{13}C NMR (400 MHz, DMSO-d_6, ppm): δ 154.37, 148.26, 142.28, 141.82, 141.68, 140.81, 125.75, 118.77, 111.24, 106.43, 102.86, 102.04, 65.52, 65.03, 64.41, 64.33.

EDOT-PSe (2). 71.0% yield. ^{1}H NMR (400 MHz, DMSO-d_6, ppm): δ 9.05 (s, 1H). 7.03 (s, 1H), 6.88 (s, 1H), 4.44 (s, 2H), 4.36 (s, 2H), 4.29 (s, 4H).

2.3.3 Representative procedures for the synthesis of 3-8. To an nitrogen-degassed solution of 11a or 11b (0.400 mmol) and 10a/10b or 10c (1.60 mmol) in dry DMF (25.0 mL) was added Pd(PPh$_3$)$_2$Cl$_2$ (0.0280 g, 0.0400 mmol) and the mixture was stirred at 95 °C for 24 h. After being cooled to room temperature, the mixture was poured into saturated aqueous brine and then extracted with dichloromethane (3 × 20.0 ml). The crude product was washed twice with water, dried over anhydrous $MgSO_4$ and purified by silica column chromatography to give 3-8.

Th-PT (3). 85.0% yield. ^{1}H NMR (400 MHz, DMSO-d_6, ppm): δ 8.99 (d, J = 2 Hz, 1H), 8.64 (dd, J = 3.6, 1H), 8.18 (dd, J = 3.2 Hz, 1H), 7.92 (d, J = 5.2 Hz, 1H), 7.83 (d, J = 5.2 Hz, 1H), 7.37-7.35 (m, 1H), 7.32-7.29 (m, 1H). ^{13}C NMR (400 MHz, DMSO-d_6, ppm): δ 154.04, 147.17, 145.37, 141.27, 140.16, 135.76, 131.43, 131.40, 129.06, 128.66, 128.08, 127.57, 119.92.

Th-PSe (4). 79.1% yield. ^{1}H NMR (400 MHz, DMSO-d_6, ppm): δ 8.78 (s, 1H), 8.65 (dd, J = 4.4, 1H), 8.11 (dd, J = 4.4 Hz, 1H), 7.85 (dd, J = 6 Hz, 1H), 7.76 (dd, J = 6 Hz, 1H), 7.29-7.31 (m, 1H), 7.23-7.25 (m, 1H). ^{13}C NMR (400 MHz, DMSO-d_6, ppm): δ 154.20, 147.46, 146.71, 146.42, 140.64, 139.91, 137.38, 135.54, 133.44, 131.79, 130.23, 128.85, 121.78.

MeTh-PT (5). 83.0% yield. ^{1}H NMR (400 MHz, DMSO-d_6, ppm): δ 8.89 (s, 1H), 8.47 (d, J = 1.2, 1H), 8.00 (d, J = 1.2 Hz, 1H), 7.49 (d, J = 0.8 Hz, 1H), 7.39 (d, J = 1.2 Hz, 1H), 2.34 (s, 3H), 2.32 (s, 3H). ^{13}C NMR (400 MHz, DMSO-d_6, ppm): δ 154.00, 147.16, 145.22, 140.94, 139.94, 139.05, 138.09, 135.51, 133.47, 129.69, 126.90, 123.96, 119.91, 15.49, 15.39.

MeTh-PSe (6). 78.0% yield. ^{1}H NMR (400 MHz, $CDCl_3$, ppm): δ 8.64 (s, 1H), 8.49 (s, 1H), 7.84 (s, 1H), 7.18 (s, 1H), 7.06 (s, 1H), 2.38 (s, 3H), 2.37 (s, 3H). ^{13}C NMR (400 MHz, DMSO-d_6, ppm): δ 162.65, 159.67, 153.99, 147.80, 140.39, 139.70, 138.75, 136.84, 134.89, 130.24, 126.92, 123.07, 122.13, 16.08, 15.98.

HexTh-PT (7). 72.0% yield. ^{1}H NMR (400 MHz, $CDCl_3$, ppm): δ 8.78 (s, 1H), 8.54 (s, 1H), 7.94 (s, 1H), 7.21 (s, 1H), 7.07 (s, 1H), 2.70 (dd, J = 22.4 Hz, 4H), 1.75-1.66 (m, 4H), 1.40-1.38 (m, 2H), 1.37-1.33 (m, 9H). ^{13}C NMR (400 MHz, DMSO-d_6, ppm): δ 155.09, 148.18, 146.24, 145.48, 144.70, 140.94, 140.33, 136.23, 133.49, 129.57, 126.34, 122.28, 120.74, 31.84, 30.80, 30.72, 30.60, 29.84, 29.18,29.15, 28.00, 26.98, 22.77, 17.68, 14.23, 13.73.

HexTh-PSe (8). 70.2% yield. ^{1}H NMR (400 MHz, $CDCl_3$, ppm): δ 8.66 (s, 1H), 8.53 (s, 1H), 7.88 (s, 1H), 7.20 (s, 1H), 7.08 (s, 1H), 2.70 (dd, J = 21.2 Hz, 4H), 1.75-1.66 (m, 4H), 1.41-1.33 (m, 12H). ^{13}C NMR (400 MHz, DMSO-d_6, ppm): δ 159.68, 154.04, 147.90, 145.35, 144.41, 141.89, 140.52, 136.80, 133.93, 129.37, 126.11, 122.31, 122.15, 31.85, 30.83, 30.73, 30.63, 29.85, 29.19, 29.16, 22.78, 14.26.

2.4 Electrochemical tests and polymerization

Electrochemical tests and polymerization of the monomers were performed in a one-compartment cell with the use of Model 263A potentiostat-galvanostat (EG&G Princeton Applied Research) under computer control. For electrochemical tests, the working and counter electrodes were both Pt wires with a diameter of 0.5 mm, respectively. To obtain a sufficient amount of the polymer films for characterization, Pt sheet was employed as the working electrode and another Pt sheet was used as the counter electrode. They were placed 5 mm apart during the examination. Prior to each experiment, these electrodes mentioned above were carefully polished with 1500 mesh abrasive paper, cleaned successively with water and acetone, and then dried in air. An Ag/AgCl electrode directly immersed in the solution served as the reference electrode, with its electrode potential calibrated against a saturated calomel electrode, and it revealed sufficient stability during the experiments. All the solutions were deaerated by a dry nitrogen stream and maintained under a slight overpressure through all the experiments to avoid the effect of oxygen.

2.5 Spectroelectrochemical and kinetic studies

Spectroelectrochemical and kinetic studies were recorded on a SPECORD 200 PLUS UV-vis spectrophotometer and the potentials were controlled using VersaSTAT3 potentiostat-galvanostat (EG&G Princeton Applied Research). A three-electrode quartz cell was utilized consisting of an Ag/AgCl electrode, a Pt wire counter electrode, and an ITO coated glass working electrode. All measurements were carried out in MeCN-Bu$_4$NPF$_6$ (0.1 mol L^{-1}).

The optical density (ΔOD) at the specific wavelength (λ_{max}) of the sample was determined by T values of electrochemically oxidized and reduced films, using the following equation:

$$\Delta OD = \log(T_{\mathrm{ox}}/T_{\mathrm{red}}) \qquad (1)$$

The coloration efficiency (*CE*) is defined as the relation between the injected/ejected charge as a function of electrode area (Q_d) and the change in optical density (ΔOD) at the specific dominant wavelength (λ) of the sample as illustrated by the following equation:

$$CE = \Delta OD/Q_\mathrm{d} \qquad (2)$$

3. RESULTS AND DISCUSSION

3.1 Monomer synthesis

The synthesis of monomers was shown in Scheme 2. Firstly, 4,7-dibromo[1,2,5]thiadiazolo[3,4-*c*]pyridine and 4,7-dibromo[1,2,5] selenadiazolo[3,4-*c*]pyridine were prepared according to modified literature procedures.[33-35,41] From these two electron-deficient acceptor units, the precursors were synthesized in satisfactory yields (typically more than 70%). The synthesis and properties of EDOT-PT and corresponding polymer has recently been published in our previous report.[35] Compared with EDOT based D-A-D monomers, thiophenes based analogues exhibit better solubility in organic solvents, which is essential for increasing the processability of the corresponding polymers.

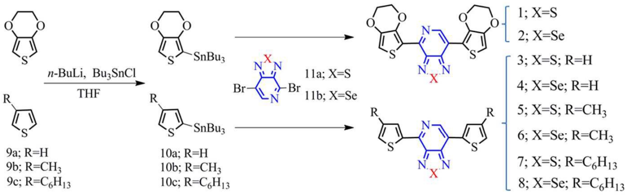

Scheme 2 Synthetic routes of PT/PSe-based D-A-D monomers. Compound: EDOT-PT (1), EDOT-PSe (2), Th-PT (3), Th-PSe (4), MeTh-PT (5), MeTh-PSe (6), HexTh-PT (7), and HexTh-PSe (8).

3.2 Optical property

In initial attempts to understand the structure-property relationships of D-A-D monomers, UV-vis spectra of these monomers were examined in CH_2Cl_2. The optical data of these monomers are summarized in Table 1. As shown in Figure 1, these monomers exhibited dual-band absorptions since this was a characteristic signature generally observed in D-A-D monomers. The absorption bands at the short wavelengths could be ascribed to π-π* transition of conjugated systems (250~370 nm),[42] while the absorption bands at long wavelengths (370~640 nm) originated from charge transfer between thiophenes and PT/PSe.[43,44]

As the donor unit changes, the absorption peaks of PT/PSe-based monomers exhibited no significant shifts in high-energy region. However, the low-energy band shifts by a greater extent than the high-energy band, and a significant red shift was observed from Th-PT/PSe to MeTh-PT/PSe to HexTh-PT/PSe, and further to EDOT-PT/PSe. The phenomenon may be ascribed to substituent groups changing the electronic configuration of conjugated systems, further turning intramolecular charge transfer.[44-46] These results clearly suggested that alkyl chain substituents would maintain the high-energy absorption band and modulate the low-energy absorption band in D-A-D systems. It is worth noting that these low-energy absorption bands distribute throughout the visible region. Therefore, the simple and feasible method to modulate electronic characteristic in the D-A-D compounds would be highly advantageous to obtain desired optical and colorimetric properties. Furthermore, the absorption bands of PSe-based monomers shifted to a longer wavelength compared with those of PT analogues, due to heavier atoms decreasing the LUMO level.[43] A similar trend is always observed in D-A-D systems based on benzothiadiazole/benzoselenadiazole units.[18]

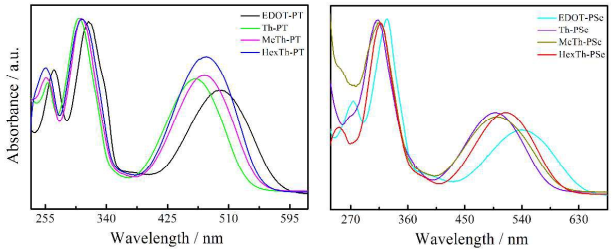

Fig. 1 Absorption spectra of PT/PSe-based D-A-D monomers in CH_2Cl_2.

From the fluorescence emission spectra of monomers examined in CH_2Cl_2 (Fig. 2), all the monomers exhibited emission peaks in the range of 603~714 nm (Table 1). In good agreement with the UV-vis spectral results, the emission spectra of PSe-based monomers displayed significant red shifts compared with their PT analogues while their overall emission region tailed off to 720~860 nm in comparison with those of PT-based monomers (710~820 nm). As the electron-donating ability of donor unit increase, a red shift of the emission spectra was observed from Th-PT to MeTh-PT to HexTh-PT, and further to EDOT-PT. However, the emission spectrum of MeTh-PSe exhibited unnatural blue shift in comparison with that of Th-PSe in PSe based system. As shown in Fig. 3, all designed monomers showed satisfied photoluminescence properties and displayed orange, red and purple emission characteristics. Moreover, the fluorescence quantum yields (Φ_F), measured by the absolute method, were 0.501, 0.072, 0.849, 0.307, 0.701, 0.200, 0.711 and 0.184 for EDOT-PT, EDOT-PSe, Th-PT, Th-PSe, MeTh-PT, MeTh-PSe, HexTh-PT, and HexTh-PSe, respectively. Compared to PSe-based monomers, PT-based monomers exhibited better emission signatures and excellent fluorescence quantum yields (0.501~0.849). Due to the bare unshared pair electrons on pyridine ring, these monomers might reveal the sensitivity to ions. Combining the relatively high quantum yield with the sensitivity to ions, these monomers probably should be considered in the rational design of fluorescent materials, such as emitters in light-emitting diodes, laser dyes and fluorescent sensors.

3.3 Electrochemical polymerization

The electrochemical properties of these monomers were examined in CH_2Cl_2-Bu_4NPF_6 (0.1 mol L^{-1}) except HexTh-PSe. Electrochemical polymerization of HexTh-PSe was performed in MeCN-Bu_4NPF_6 (0.1 mol L^{-1}), due to the good solubility of as-formed polymer in CH_2Cl_2.

Table 1 Electrochemical and optical data for PT/PSe-based D-A-D monomers

monomers	$E_{m,ox}$ (V)	$\lambda_{max,1}$ (nm)	$\lambda_{max,2}$ (nm)	$\lambda_{max,3}$ (nm)	λ_{em} (nm)	HOMO (eV)^a	LUMO (eV)^b	$E_{g,opt}$ (eV)^c
EDOT-PT	0.88	266	315	500	653	-5.68	-3.54	2.14
EDOT-PSe	0.81	274	328	542	714	-5.61	-3.67	1.94
Th-PT	1.24	258	302	464	603	-6.04	-3.73	2.31
Th-PSe	1.10	270	313	498	643	-5.90	-3.59	2.13
MeTh-PT	1.01	256	305	476	615	-5.81	-3.56	2.25
MeTh-PSe	1.00	253	316	502	613	-5.80	-3.74	2.06
HexTh-PT	1.15	255	307	479	618	-5.95	-3.71	2.24
HexTh-PSe	1.05	252	317	515	648	-5.85	-3.80	2.05

The HOMO energy levels were determined by ^{a}HOMO = -($E_{m,ox}$ + 4.80) (eV). $^c E_{g,opt} = 1240/\lambda_{onset}$ (eV), ^{b}LUMO = HOMO + $E_{g,opt}$. $E_{m,ox}$ and $E_{g,opt}$ are the onset oxidation potential and optical bandgap of the monomer, respectively.

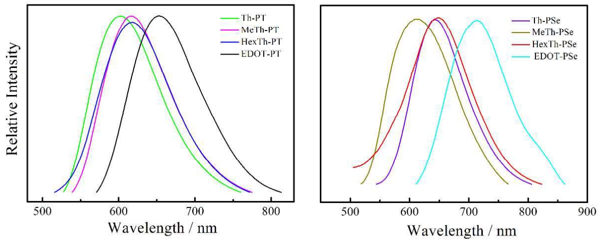

Fig. 2 Emission spectra of PT/PSe-based D-A-D monomers as indicated in CH_2Cl_2.

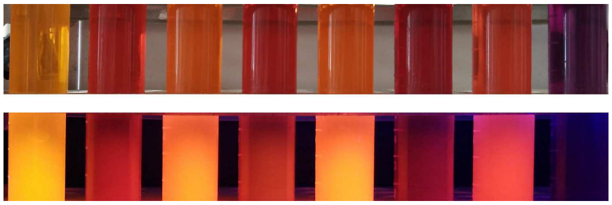

Fig. 3 Photoluminescence of the PT/PSe-based D-A-D monomers in CH_2Cl_2 under 365 nm UV irradiation (left to right: Th-PT, Th-PSe, MeTh-PT, MeTh-PSe, HexTh-PT, HexTh-PSe, EDOT-PT, and EDOT-PSe,).

From their anodic oxidation behaviors (Fig. S1 and Table 1), the initial oxidation of PSe based monomers (0.81~1.10 V) was observed at lower potentials than those of corresponding PT analogues (0.88~1.24 V), which confirms that PSe based D-A-D systems are electron richer than PT-based systems.[21,37,47] In terms of donor units and steric hindrance of substituents on the structure-property relationships, PT-based monomers exhibited the following oxidation onset potential ($E_{m,ox}$) trend: EDOT-PT (0.88 V) < MeTh-PT (1.01 V) < HexTh-PT (1.15 V) < Th-PT (1.24 V). From these results, it can be seen that EDOT-PT had the lowest oxidation onset potential among PT-based monomers, which was mainly attributed to the stronger electron-donating ability of EDOT compared to alkyl thiophenes.[48,49] The oxidation onset potential for MeTh-PT is 0.13 V less than Th-PT, which can be ascribed to electron-donating ability of alkyl chain. Hexyl chain was electron richer relative to methyl group, but HexTh-PT exhibited the relatively high oxidation onset potential. The phenomenon was mainly attributable to significant steric hindrance in large alkyl chain.[5,10] Therefore, substituents affect the electrochemical performance of these monomers not only through modulating electronic nature but by changing steric hindrance. In addition, PSe-based monomers also follow similar trend in terms of oxidation onset potentials (from low to high): EDOT-PSe (0.81 V) < MeTh-PSe (1.00 V) < HexTh-PSe (1.05 V) < Th-PSe (1.10 V).

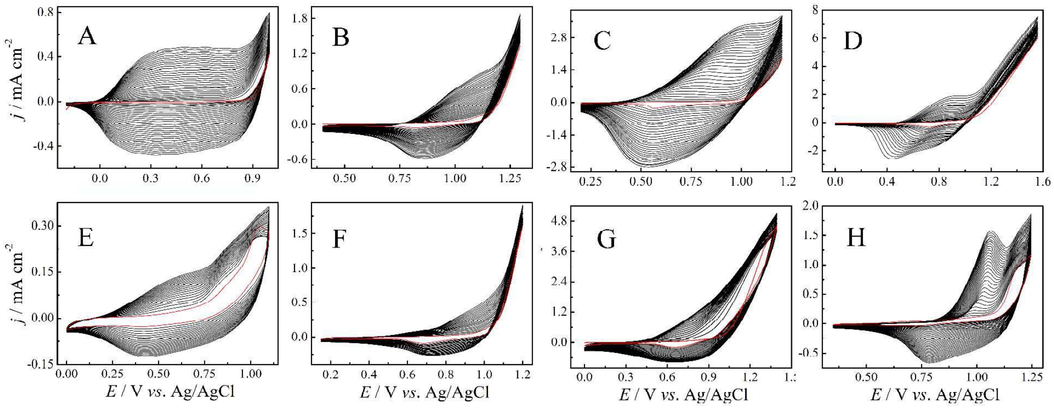

Fig. 4 CVs of the electropolymerization of 5 mmol L^{-1} EDOT-PT (A), Th-PT (B), MeTh-PT (C), HexTh-PT(D), EDOT-PSe (E), Th-PSe (F) and MeTh-PSe (G) in CH_2Cl_2-Bu_4NPF_6 (0.10 mol L^{-1}) and 5 mmol L^{-1} HexTh-PSe (H) in MeCN-Bu_4NPF_6 (0.10 mol L^{-1}) on a Pt working electrode, respectively. Potential scan rate: 100 mV s^{-1}.

Potentiodynamic electropolymerization of these monomers was performed in the electrolytic system, as shown in Fig. 4. During the experimental process, current densities in CVs grew uniformly, which was characteristic of the increase of polymers on the electrode. Because of increased conjugated polymer attaching on the electrode, the anodic and cathodic peak potentials shifted, and additional potential meant to balance the electrical resistance corresponding to increased polymer.[50-51] Also, these polymers exhibited broad redox waves, which may be attributed to the polymer with different chain lengths and the transition of conductive species on conjugated block.[51,53] Fig. 4 also revealed that the presence of substituent groups on donor units influenced the redox behavior of the electrodeposited polymers, resulting in sharp redox peaks with increasing alkyl chain length. Furthermore, there is a difference in the oxidation peak current density (from low to high): EDOT-PT (0.49 mA cm^{-2}, the 20th cycle, the same below) < Th-PT (1.09 mA cm^{-2}) < HexTh-PT (1.89 mA cm^{-2}) < MeTh-PT (3.40 mA cm^{-2}); EDOT-PSe (0.15 mA cm^{-2}) < Th-PSe (0.44 mA cm^{-2}) < MeTh-PSe (1.55 mA cm^{-2}) < HexTh-PSe (1.58 mA cm^{-2}). The phenomenon could be ascribed to the interdigitation of alkyl chains attached on thiophene ring, which is beneficial to the formation of high quality film.

3.4 Structural characterization

The polymerization of these monomers (excluding Th-PT/PSe monomers) would only happen at C_α of thiophene rings considering radical cation mechanism of electropolymerization. For Th-PT/PSe, the polymerization may occur at both C_α and C_β positions.

To further elucidate these conjugated structures and interpret the polymerization mechanism, FT-IR spectra of these monomers and polymers were recorded, as illustrated in Fig. S2~S3. The detailed peak assignments are summarized in Table S1-S4. From these results, the peaks at around 1200 and 860 cm^{-1} in the spectra of the monomers can be attributed to =C–H in-plane and out-of-plane deformation vibrations of thiophene rings, respectively. The peaks at around 3080 cm^{-1} are characteristic for the =C–H vibration of thiophene rings. However, all the peaks mentioned above disappear/weaken in the spectra of their polymers, demonstrating that these monomers are electropolymerized mainly through the coupling at C_α positions. Additionally, the strong absorption peaks at 840 cm^{-1} are typical signals for the incorporation of dopants, namely PF_6^- ions.

3.5 Electrochemistry of polymers

To obtain a deep understanding into the electrochemical behaviors of these polymers, the electrochemistry of polymers in monomer-free MeCN-Bu_4NPF_6 (0.1 mol L^{-1}) was explored by cyclic voltammetry (CV). The obtained results were displayed in Fig. 5~6. All the polymers exhibited broad redox waves, in good agreement with the results for potentiodynamic electropolymerization of monomers (Fig. 4). Besides, the redox peak current densities were proportional to potential scan rates, demonstrating that electoactive films were attached to the electrode and their redox behaviors were controlled non-diffusionally. Furthermore, an obvious hysteresis can be observed in their redox processes (Fig. 5~6), which probably could be accounted for these reasons: (1) slow interfacial electron transfer through solution/polymer and polymer/electrode; (2) slow mutual transition of various conductive species; (3) the rearrangement of polymer block during the doping/dedoping processes.[53,55,56] With the elongation of alkyl chain length, the corresponding polymer exhibited sharper redox peaks in comparison with that of P Th-PT/PSe, implying faster doping/dedoping processes of alkyl thiophenes based polymers. This phenomenon probably result from the steric hindrance from the alkyl chains, which causes the polymer chains to separate from each other.[52] The separation generally promotes a more expanded morphology and facilitates the transport of counterbalancing ions across the conjugated block, and thus usually favors fast switching of conjugated polymers.[1,4]

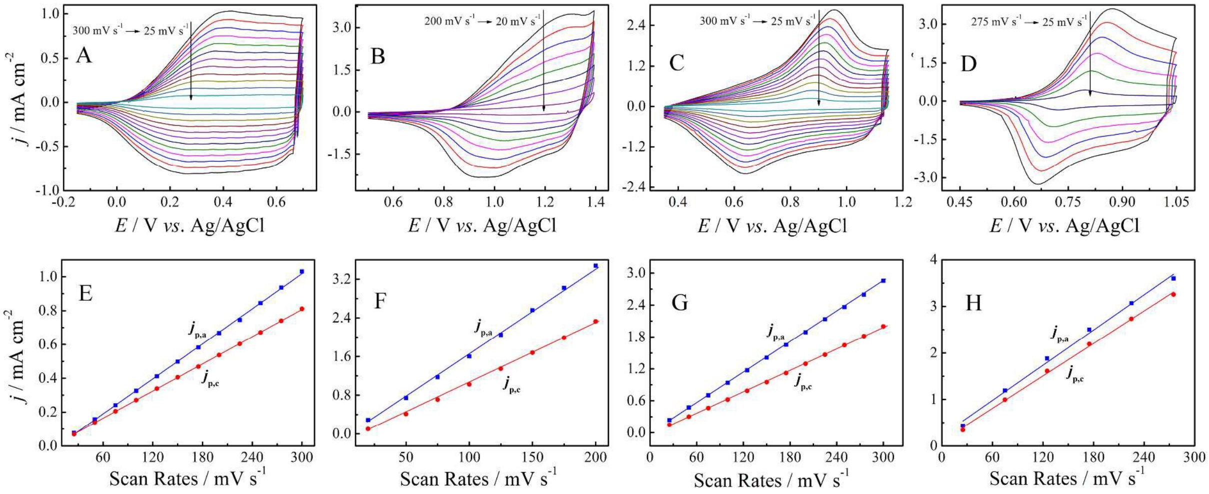

Fig. 5 CVs of PEDOT-PT (A), PTh-PT (B), PMeTh-PT (C), and PHexTh-PT(D) modified Pt electrodes in monomer-free MeCN-Bu_4NPF_6 (0.10 mol L^{-1}) at different potential scan rates and the relationship of anodic ($j_{p,a}$) and cathodic ($j_{p,c}$) peak current densities *vs.* scan rates between the neutral and oxidized states of PEDOT-PT (E), PTh-PT (F), PMeTh-PT (G), and PHexTh-PT(H).

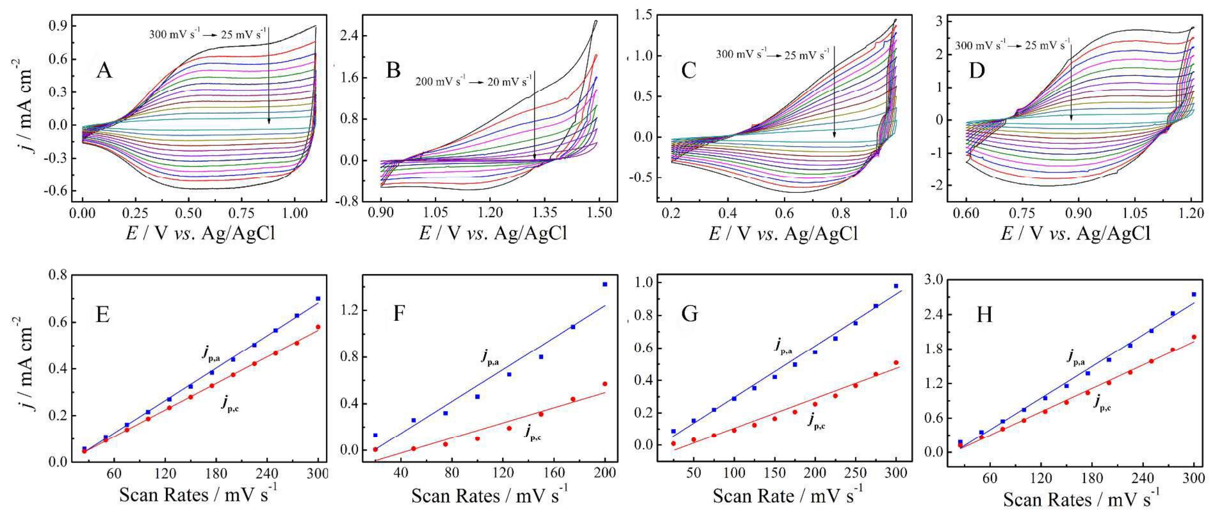

Fig. 6 CVs of PEDOT-PSe (A), PTh-PSe (B), PMeTh-PSe (C), and PHexTh-PSe (D) modified Pt electrodes in monomer-free MeCN-Bu_4NPF_6 (0.10 mol L^{-1}) at different potential scan rates and the relationship of anodic ($j_{p,a}$) and cathodic ($j_{p,c}$) peak current densities *vs.* scan rates between the neutral and oxidized states of PEDOT-PSe (E), PTh-PSe (F), PMeTh-PSe (G), and PHexTh-PSe (H).

3.6 Spectroelectrochemistry

Spectroelectrochemical properties were explored by using the changes in optical absorption spectra under voltage pulses. Optical absorption spectra of these polymers electrodeposited on ITO-coated glasses were recorded in monomer-free MeCN-Bu_4NPF_6 (0.10 mol L^{-1}) from the neutral state to oxidized state (Fig. 7). It is observed that both the donor and acceptor units in these conjugated systems influence the absorption spectra of the polymers to some extent.

In accordance with the absorption of these monomers, the corresponding polymers exhibited dual-band absorptions (Fig. 7) in the neutral state and the absorption band at longer wavelength was attributed to the intramolecular charge transfer. The absorption peaks of neutral polymers red-shifted relative to their corresponding monomers, due to their increased conjugated blocks. Red-shifted absorption bands are also an evidence that the polymer backbone was highly rigid, planar and effectively π-conjugated.[1,4] Furthermore, the band gaps (E_g) of these D-A-D polymers were calculated from the onset of the low energy end of charge transfer as 1.12 eV (PEDOT-PT), 1.09 eV (PEDOT-PSe), 1.75 eV (PTh-PT), 1.51 eV (PTh-PSe), 1.38 eV (PMeTh-PT), 1.34 eV (PMeTh-PSe), 1.47 eV (PHexTh-PT), and 1.54 eV (PHexTh-PSe).

Among them, the entire absorption bands of PSe-based polymers except for PHexTh-PSe shifted to the lower energy region compared with PT-based polymers. As a consequence, a band gap reduction was observed for PSe-based polymers owing to the substitution of heavier Se, which decreased the LUMO levels of these polymers.[43,44] Furthermore, due to enhanced interchain packing of polymer chains caused by alkyl substituents on thiophene rings and raising their subtle electronic changes on the conjugated block, the entire absorption spectra of PMeTh-PT/PSe and PHexTh-PT/PSe are red-shifted in compared with PTh-PT/PSe.[45,46] In concert with their results of electropolymerization behavior, the absorption spectra of PHexTh-PT/PSe blue-shifted in comparison with that of PMeTh-PT/PSe due to the increased strain of the longer hexyl group.

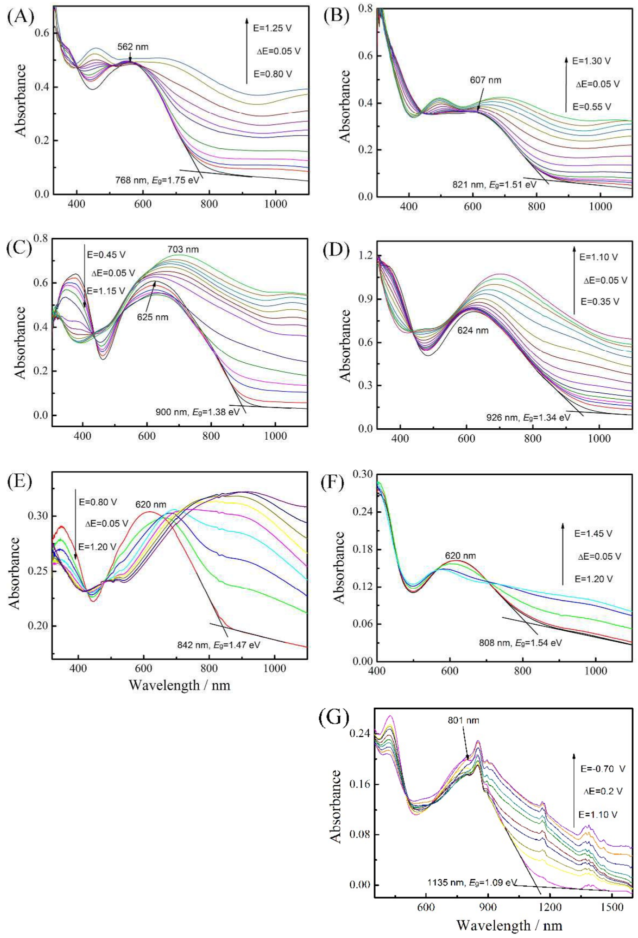

Fig. 7 Spectroelectrochemistry of PTh-PT (A), PTh-PSe (B), PMeTh-PT (C), PMeTh-PSe (D), PHexTh-PT(E), PHexTh-PSe (F), and PEDOT-PSe (G) on ITO-coated glasses in monomer-free MeCN-Bu_4NPF_6 (0.1 mol L^{-1}).

Table 2 CIE color coordinates of PT/PSe-based D-A-D polymers

	CIE	PEDOT-PT	PTh-PT	PMeTh-PT	PHexTh-PT	PEDOT-PSe	PTh-PSe	PMeTh-PSe	PHexTh-PSe
Neutral state	L*\a*\ b*	57.80\ -30.96\ 19.11	65.99\ 11.27\ -10.04	58.30\ -3.27\ -23.36	87.76\ 2.47\ -9.26	89.98\ -5.15\ 7.12	57.21\ 4.29\ -7.59	70.20\ -6.60\ -6.01	94.38\ 1.49\ -7.03
Oxidized state	L*\a*\ b*	56.15\ -3.92\ -14.87	67.65\ 11.90\ -4.76	58.95\ -1.56\ -22.27	87.66\ 2.54\ -8.10	88.35\ -2.13\ -3.86	56.98\ 4.81\ -8.40	60.62\ -0.83\ -4.57	84.64\ 2.55\ -6.80

In addition, visual observation during the electrochromic tests demonstrated that these PT/PSe-based D-A-D polymers in the neutral state displayed a wide range of colors, including green, purple, gray, sky blue, and dark blue (as shown in Table 2~3), providing more plentiful electrochromic colors. As the applied potential increased, the absorption bands of PEDOT-PSe at 433 and 846 nm started to decrease with a polaron absorption increasing in the near-infrared region. These changes in the absorption spectra were accompanied with color changes from green (L^*=89.98; a^*=-5.15; b^*=7.12) to blue (L^*=88.35; a^*=-2.13; b^*=-3.86) (Table 2~3). Interestingly, PTh-PT/PSe, PMeTh-PT/PSe and PHexTh-PT/PSe showed significant absorption changes between the neutral and oxidized states in near-infrared region, but few change was observed in the visible range. Under different applied voltages, the colors of these electrochromic polymers remain constant (Table 2~3). A possible explanation for this phenomenon may depend on the intrinsic characteristic of chalcogenodiazolo[3,4-*c*]pyridine based D-A-D polymers. The intriguing features of these polymeric materials indicated that inserting chalcogenodiazolo[3,4-*c*]pyridine into D-A-D systems might allow near-infrared electrochromic materials.

To gain a greater understanding of the near-infrared electrochromic application, the CIE 1976 ($L^*a^*b^*$) color coordinates and photographs were determined in which L^* is the parameter of the lightness (0 = black, 100 = diffuse white), a^* is the red-green balance and b^* is the yellow-blue balance. As shown in Table 3, the CIE color coordinates of these electrochromic polymers remain relatively constant under different applied voltages, in agreement with visual colors.

Table 3 Photographs of PT/PSe-based D-A-D polymers

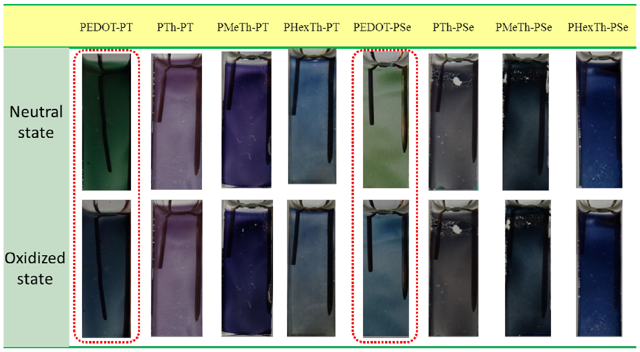

3.7 Kinetic studies

To investigate these electrochromic polymers in more detail, the optical switching studies of PEDOT-PT/PSe, PTh-PT/PSe, PMeTh-PT/PSe and PHexTh-PT/PSe were carried out using optical spectroscopy combining with the double step chronoamperometry method. Typical electrochromic parameters of these polymers upon switching between the neutral and oxidized states, including optical contrast, coloration efficiency, and response time, were summarized in Table S5~S11.

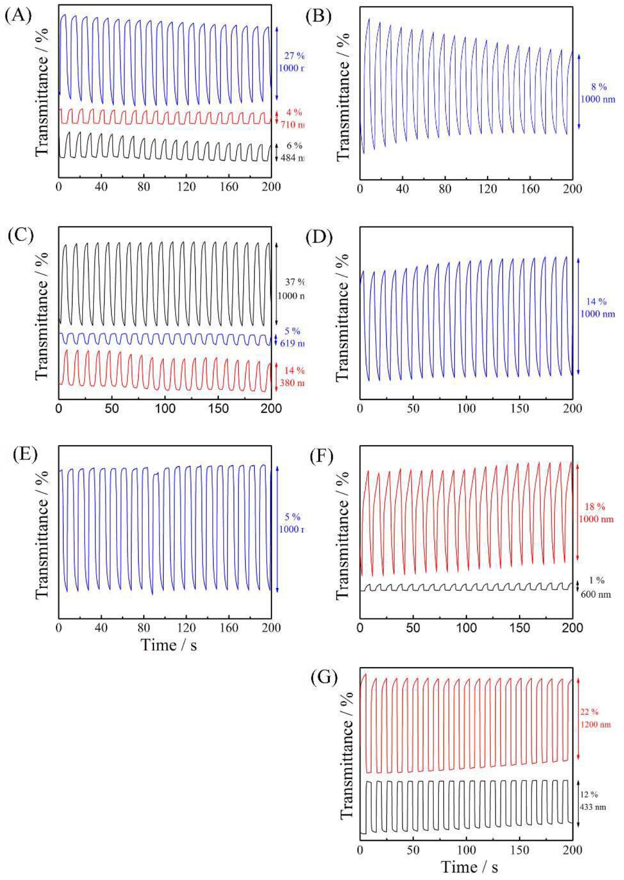

Fig. 8 Transmittance-time profiles of these polymers recorded during double step spectrochronoamperometry. Switching time: 5 s. A: PTh-PT between 0.80~1.25 V; B: PTh-PSe between 0.55~1.30 V; C: PMeTh-PT between 0.45~1.15 V; D: PMeTh-PSe between 0.35~1.10 V; E: PHexTh-PT between 0.80~1.20 V; F: PHexTh-PSe between 1.20~1.45 V; G: PEDOT-PSe between -0.70~1.10 V.

For PEDOT-PSe, the optical contrast ratios between neutral (at -1.0 V) and oxidized states (at 1.0 V) were calculated to be 12 % at 433 nm and 22 % at 1200 nm (Fig. 8), respectively. These electrochromic parameters of PEDOT-PSe were inferior to those of PEDOT-PT (28% at 431 nm; 5% at 746 nm; 51% at 1337 nm).[32] It is clearly seen from the transmittance curves in Fig. 8 that PTh-PT/PSe, PMeTh-PT/PSe and PHexTh-PT/PSe displayed substandard optical contrast ratios in the visible range and kept their color constant under different applied voltages. However, these obtained polymers show superior optical contrast (~37%) in the near-infrared region compared with that in the visible region, hence promoting the perspectives for near-infrared electrochromic materials.

Also, response time is an important parameter of electrochromics, and contributed to commercial applications. Clearly, these obtained polymers exhibited fast response time (0.3~4 s) in the oxidation and reduction processes, as shown in Table S5~S11. In particular, PEDOT-PSe achieved 95% of its optical contrast in 0.50 s at 433 nm and 0.30 s at 1200 nm during the oxidized process, while the response time was 0.45 s at 433 nm and 0.60 s at 1200 nm during the reduced process. Compared with benzoselenadiazole system 4,7-di-2,3-dihydrothieno[3,4-*b*][1,4]dioxin-5-yl-2,1,3-benzoselenadiazole (1.7~5.6 s),[13,21] PEDOT-PSe exhibited further faster switching times (0.3~0.6 s), primarily due to the ease of diffusion of counterbalancing ion across PEDOT-PSe film.

3.8 Stability

Redox stability, related to aspects involved to the utilization and energy consumption during application process, is an important requirement for electrochromic materials. Therefore, these designed polymers were constructed into single electrochromic devices, and long-term redox stability of these electrochromic devices (ECDs) was investigated. The construction of a polymer electrochromic device was present in Fig. S4, where an ITO-coated glass slide was covered with the designed electrochromic polymer as active material, and another ITO-coated glass was regarded as the transparent electrode. The device was prepared by a face-to-face placing of the ITO-coated glasses. An electrolyte layer was applied between the polymeric electrochromic layer and ITO-coated glass slide. These ECDs exhibited different redox stability, which was largely related to the structure of these obtained D-A-D polymers. PHexTh-PT, PEDOT-PT, PEDOT-PSe and PMeTh-PT ECDs displayed better stability, with 91%, 87%, 83% and 63% of the exchange charge still remaining after sweeping 1000 cycles, respectively (Fig. S5). However, the exchange charge of PMeTh-PSe, PHexTh-PSe and PTh-PT ECDs kept only 80%, 71% and 55% after 500 cycles, respectively (Fig. S5). Unfortunately, the PTh-PSe ECD revealed inferior stability and lost its electroactivity after a few cycles. In general, these obtained ECDs showed good redox stability, however, the stability of ECDs was lower than that of thiophenes based polymers.

4. Conclusion

In summary, a series of PT/PSe in alternation with a variety of thiophenes based D-A-D monomers were synthesized and their electrochemical polymerization was reported. The structure-property relationships of the monomers and electrosynthesized conjugated polymers, including optoelectronic and electrochromic properties, were systematically investigated. Overall, these donor and acceptor units played key roles on the redox behavior, band gap, optical absorption, and fluorescence of the system. These obtained polymers provided more plentiful electrochromic color with a wide range of green, purple, gray, sky blue and dark blue. In particular, PEDOT-PSe exhibited a color change from green to sky blue and revealed faster response time (0.3~0.6 s) compared to benzoselenadiazole system 4,7-di-2,3-dihydrothieno[3,4-*b*][1,4]dioxin-5-yl-2,1,3-benzoselenadiazole (1.7~5.6 s) and favorable efficiencies (~174 cm^2/C). Furthermore, PTh-PT/PSe, PMeTh-PT/PSe and PHexTh-PT/PSe showed satisfactory electrochromic performance including superior optical contrast (~37%) in the near-infrared region and fast response time (0.4~4 s), and kept color constant under different applied voltages. Based on these preliminary results, intriguing features of these polymeric materials and panoramic breadth of the colors further confirm that inserting chalcogenodiazolo[3,4-*c*]pyridine into D-A-D system allows colorful near-infrared electrochromes.

Acknowledgments

We are grateful to the National Natural Science Foundation of China (grant number: 51303073, 51463008), Ganpo Out-standing Talents 555 projects (2013), the Training Plan for the Main Subject of Academic Leaders of Jiangxi Province (2011), the Natural Science Foundation of Jiangxi Province (grant number: 20122BAB216011 and 20142BAB216029), the Science and Technology Landing Plan of Universities in Jiangxi province (KJLD12081), Provincial Projects for Postgraduate Innovation in Jiangxi (YC2014-S441, YC2014-S431), and Scientific Research Projects of Jiangxi Science & Technology Normal University (2014QNBJRC003) for their financial support of this work.

References

1 P. M. Beaujuge and J. R.Reynolds, *Chem. Rev.*, 2010, **110**, 268-320.
2 P. M. Beaujuge, C. M. Amb and J. R. Reynolds, *Acc. Chem. Res.* 2010, **43**, 1396-1407.
3 L. Groenendaal, G. Zotti, P. Aubert, S. M. Waybright and J. R. Reynolds, *Adv. Mater.,* 2003, **15**, 855-879.
4 G. Gunbas and L. Toppare, *Chem. Commun.,* 2012, **48**, 1083-1101.
5 L. Beverina, G. A. Pagani and M. Sassi, *Chem. Commun.*,2014, **50**, 5413-5430.
6 C. M. Amb, A. L. Dyer and J. R. Reynolds, *Chem. Mater.,* 2011, **23**, 397-415.
7 G. Nie, L. Zhou and H. Yang, *J. Mater. Chem.*, 2011, **21**, 13873-13880.
8 G. Nie, L. Zhou, Q. Guo and S. Zhang, *Electrochem. Commun*, 2010, **12**, 160-163.
9 C. Li, C. Liu, L. Shi and G. Nie, *J. Mater. Sci.*, 2015, **50**, 1836-1847.
10 J. A. Kerszulis, K. E. Johnson, M. Kuepfert, D. Khoshabo, A. L. Dyer and J. R. Reynolds, *J. Mater. Chem. C,* 2015, **3**, 3211-3218.
11 G. Sonmez, C. K. F. Shen, Y. Rubin and F. Wudl, *Angew. Chem.*, 2004, **116**, 1524-1528.
12 M. İçli, M. Pamuk, F. Algi, A. M. Önal and A. Cihaner, *Chem. Mater.,* 2010, **22**, 4034-4044.
13 A. Durmus, G. E. Gunbas, P. Camurlu and L. Toppare, *Chem. Commun.,* 2007, 3246-3248.
14 F. Algi and A. Cihaner, *Org. Electron.* 2009, **10**, 704-710.
15 P. M. Beaujuge, S. Ellinger and J. R. Reynolds, *Adv. Mater.,* 2008, **20**, 2772-2776.
16 A. Durmus, G. E. Gunbas and L. Toppare, *Chem. Mater.,* 2007, **19**, 6247-6251.

17 S. Celebi, A. Balan, B. Epik, D. Baran and L. Toppare, *Org. Electron.* 2009, **10**, 631-636.

18 Ş. Özdemira, A. Balana, D. Barana, Ö. Doğana and L. Topparea, *React. Funct. Polym.,* 2011, **71**, 168-174.

19 S. Tarkuc, Y. A. Udum and L. Toppare, *Polymer*, 2009, **50**, 3458-3464.

20 Z. Xu, M. Wang, J. Zhao, C. Cui, W. Fan and J. Liu, *Electrochim. Acta,* 2014, **125**, 241-249.

21 A. Cihaner and F. Algi, *Adv, Funct. Mater.,* 2008, **18**, 3583-3589.

22 G. E. Gunbas, A. Durmus and L. Toppare, *Adv. Mater.,* 2008, **20**, 691-695.

23 G. E. Gunbas, A. Durmus and L. Toppare, *Adv. Funct. Mater.,* 2008, **18**, 2026-2030.

24 M. Nikolou, A. L. Dyer, T. T. Steckler, E. P. Donoghue, Z. Wu, N. C. Heston, A. G. Rinzler, D. B. Tanner and J. R. Reynolds, *Chem. Mater.,* 2009, **21**, 5539-5547.

25 E. Karabiyik, E. Sefer, F. B. Koyuncu, M. Tonga, E. Özdemir, S. Koyuncu and S. Koyuncu, *Macromolecules,* 2014, **47**, 8578-8584.

26 H. Zhao, Y. Wei, J. Zhao and M. Wang, *Electrochim. Acta,* 2014, **146**, 231-241.

27 Cheng, Y.-J.; Yang S.-H.; Hsu, C.-S. *Chem. Rev*. 2009, **109**, 5868-5923.

28 P. M. Beaujuge, S. Ellinger and J. R. Reynolds, *Nat. Mater.,* 2008, **7**, 795-799.

29 M. İçlia, M. Pamukb, F. Algıb, A. M. Önala and A. Cihanerc, *Org. Electron,* 2010, **11**, 1255-1260.

30 G. Öktem, A. Balan, D. Baran and L. Toppare, *Chem. Commun.,* 2011, **47**, 3933-3935.

31 T. T. Steckler, P. Henriksson, S. Mollinger, A. Lundin, A. Salleo and M. R. Andersson, *J. Am. Chem. Soc.* 2014, **136**, 1190-1193.

32 H. Zhou, L. Yang, S. C. Price, K. J. Knight and W. You, *Angew. Chem.,* 2010, **122**, 8164-8167.

33 N. Blouin, A. Michaud, D. Gendron, S. Wakim, E. Blair, R. Neagu-Plesu, M. Belletête, G. Durocher, Y. Tao and M. Leclerc, *J. Am. Chem. Soc.,* 2008, **130**, 732-742.

34 Y. Sun, S.-C. Chien, H.-L. Yip, Y. Zhang, K.-S. Chen, D. F. Zeigler, F.-C. Chen, B. Lin and A. K. Y. Jen, *J. Mater. Chem.,* 2011, **21**, 13247-13255.

35 S. Ming, S. Zhen, K. Lin, L. Zhao, J. Xu and B. Lu, *ACS Appl. Mater. Interfaces,* 2015, **7**, 11089-11098.

36 X. Zhang, W. Ying, W. Wu, J. Li and J. Hua, *Acta Chim. Sinica,* 2015, **73**, 272-280.

37 A. Patra and M. Bendikov, *J. Mater. Chem.,* 2010, **20**, 422-433.

38 B. Lu, S. Zhen, S. Zhang, J. Xu and G. Zhao, *Polym. Chem.,* 2014, *5*, 4896-4908.

39 B. Lu, S. Chen, J. Xu and G. Zhao, *Synthetic Met.,* 2013, **183**, 8-15.

40 A. Patra, Y. H. Wijsboom, G. Leitus and M. Bendikov, *Chem. Mater.,* 2011, **23**, 896-906.

41 S. Xu, Y. Liu, J. Li, Y. Wang and S. Cao, *Polym. Adv. Technol.,* 2010, **21**, 663-668.

42 E. Wang, M. Wang, L. Wang, C. Duan, J. Zhang, W. Cai, C. He, H. Wu and Y. Cao, *Macromolecules* 2009, **42**, 4410-4415.

43 G. L. Gibson, T. M. McCormick and D. S. Seferos, *J. Am. Chem. Soc.,* 2012, **134**, 539-547.

44 M. İçli-Özkut, H. İpek, B. Karabay, A. Cihaner and A. M. Önal, *Polym. Chem.,* 2013, **4**, 2457-2463.

45 E. G. Wang, C. Li, W. L. Zhuang, J. B. Peng and Y. Cao, *J. Mater. Chem.,* 2008, **18**, 797-801.

46 D. Aldakov, M. A. Palacios and P. Anzenbacher, *Chem. Mater.,* 2005, **17**, 5238-5241.

47 P. B. Pati and S. S. Zade, *Cryst. Growth Des.,* 2014, **14**, 1695-1700.

48 A. L. Dyer, M. R. Craig, J. E. Babiarz, K. Kiyak and J. R. Reynolds, *Macromolecules,* 2010, **43**, 4460-4467.

49 J. A. Kerszulis, C. M. Amb, A. L. Dyer and J. R. Reynolds, *Macromolecules,* 2014, **47**, 5462-5469.

50 T. A. Skotheim, Handbook of Conducting Polymer. New York: Marcel Dekker, 1986.

51 T. A. Skotheim, R. L. Elsembaumer and J. R. Reynolds, Handbook of Conducting Polymer, second edition. New York: Marcel Dekker, 1998.

52 J. Roncali, *Chem. Rev.,* 1992, **92**, 711-738.

53 W. Chen and G. Xue, *Prog. Polym. Sci.* 2005, **30**, 783-811.

54 S. X. Deng and R. C. Advincula, *Chem. Mater*., 2002, **14**, 4073-4080.

55 M. Li, Y. Sheynin, A. Patra and M. Bendikov, *Chem. Mater.,* 2009, **21**, 2482-2488.

56 G. Inzelt, M. Pineri, J. W. Schultze and M. A. Vorotyntsev, *Electrochim. Acta,* 2000, **45**, 2403-2421.

Graphical Abstract:

Chalcogenodiazolo[3,4-*c*]pyridine based Donor-Acceptor-Donor Polymers for Green and Near-Infrared Electrochromics

Shouli Ming, Shijie Zhen, Ximei Liu, Kaiwen Lin, Hongtao Liu, Yao Zhao, Baoyang Lu* and Jingkun Xu*

School of Pharmacy, Jiangxi Science and Technology Normal University, Nanchang 330013

*: Corresponding authors. Tel: 86-791-88537967, Fax: 86-791-83823320.

Email: lby1258@163.com; xujingkun@tsinghua.org.cn.

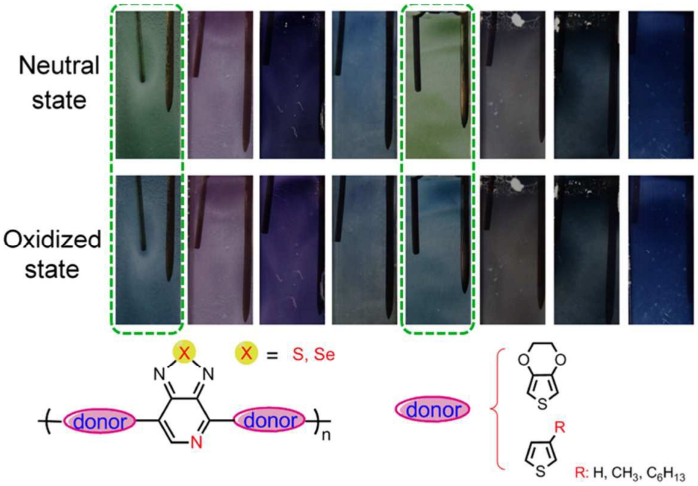

Graphical Abstract

Thiadiazolo[3,4-*c*]pyridine and selenadiazolo[3,4-*c*]pyridine were employed for rational design of novel donor-acceptor-type systems to yield neutral green and colorful near-infrared electrochromic polymers. In particular, EDOT based polymers revealed obvious color change from green to blue with faster response time (0.3~0.6 s) relative to benzochalcogenodiazole system. Furthermore, alkyl groups played key

roles on the optical absorption, leading to the neutral electrochromic polymers with different colors including purple, gray, sky blue and dark blue. Herein, the thiophene and alkyl thiophene based polymers keep color constant under different applied voltages and show superior optical contrast (~37%) in near-infrared region compared to that in visible region.